Environmental Science & Technology

Article

Pb(II) binding to humic substances: an equilibrium and spectroscopic study

Siliva Orsetti, José Luis Marco-Brown, Estela María Andrade, and Fernando Victor Molina

Environ. Sci. Technol., **Just Accepted Manuscript** • Publication Date (Web): 27 Jun 2013

Just Accepted

Environmental Science & Technology is published by the American Chemical Society.
1155 Sixteenth Street N.W., Washington, DC 20036

Pb(II) binding to humic substances: an equilibrium and spectroscopic study

*Silvia Orsetti†, Jose L. Marco-Brown, Estela M. Andrade and Fernando V. Molina**

AUTHOR ADDRESS: Instituto de Química Física de Materiales, Ambiente y Energía (INQUIMAE), y Departamento de Química Inorgánica, Analítica y Química Física, Facultad de Ciencias Exactas y Naturales, Universidad de Buenos Aires, Buenos Aires, Argentina

AUTHOR EMAIL ADDRESS: fmolina@qi.fcen.uba.ar

BRIEF: Pb(II) is proposed to bind to humic substances in two ways: a relatively strong multiligand complex leading to humic aggregation, and a weaker 1:1 complex.

CORRESPONDING AUTHOR FOOTNOTE: INQUIMAE, Facultad de Ciencias Exactas y Naturales. Ciudad Universitaria, pabellon II, C1428EHA Buenos Aires, Argentina. Tel.: +54-11-4576-3378/80 ext 230. FAX: +54-11-4576-3341. E-mail: fmolina@qi.fcen.uba.ar

†Present address: Institut für Geowissenschaften, Zentrum für angewandte Geowissenschaften, Eberhard-Karls Universität Tübingen, Germany

ABSTRACT

The binding of Pb(II) to humic acids is studied through an approach combining equilibrium and spectroscopic measurements. The methods employed are potentiometric and fluorometric titrations, fluorescence excitation-emission matrices (EEM) and IR spectroscopy. Potentiometric titration curves are analyzed using the NICA equations and an electrostatic model treating the humic particles as an elastic polyelectrolyte network. EEMs are analyzed using parallel factor analysis, decomposing the signal in its independent components and finding their dependence on Pb(II) activity. Potentiometric results are consistent with bimodal affinity distributions for Pb(II) binding, whereas fluorometric titrations are explained by monomodal distributions. EEM analysis is consistent with three independent components in the humic fluorescence response, which are assigned to moieties with different degree of aromaticity. All three components show a similar quenching behavior upon Pb(II) binding, saturating at relatively low Pb(II) concentrations. This is attributed to metal ion induced aggregation of humic molecules, resulting in the interaction between the aromatic groups responsible for fluorescence; this is also consistent with IR spectroscopy results. The observed behavior is interpreted considering that initial metal binding (observed as strongly binding sites), correspond to bi- or multidentate complexation to carboxylate groups, including binding between groups of different humic molecules, promoting aggregation; further metal ions (observed as weakly binding sites) bind to single ligand groups.

KEYWORDS Potentiometric titration; fluorescence spectroscopy; IR spectroscopy; metal-humic binding; affinity spectra.

Introduction

Humic substances (HS) are important components of natural organic matter (NOM) in groundwater and soils[1,2] HS interact with other chemical species in the natural environment, in particular binding heavy metal cations.[3–5] Among different experimental studies, equilibrium binding data, usually titration curves, have been reported and modeled.[3,6–8] Recently, the electrostatic behavior of HS was treated through the elastic polyelectrolyte network model (EPN)[9] which allows for expansion and shrinking as the HS charge changes; it can be combined with the NICA[10] intrinsic isotherm, resulting in the NICA-EPN model which has been applied to proton binding to HS.[9] Fluorescence spectroscopy is an useful tool in the study of metal binding to HS.[4,11] In the last years, excitation-emission matrix (EEM) fluorescence spectroscopy with parallel factor analysis (PARAFAC) was successfully applied for the identification and characterization of NOM.[12–16] For simple mixtures, PARAFAC components are identified with individual fluorophores present; for HS, the identified components represent fluorescence phenomena, which may be individual fluorophores or approximations to the effects of local processes such as intramolecular charge transfer.

Even after many research efforts, the exact nature of HS and the way in which they interact with metal cations remains unclear. With the aim of gaining insight in this problem, the binding of Pb(II) to humic acids (HA) is studied here by a combined analysis of titration and spectroscopic experiments. Equilibrium curves are obtained through potentiometric titrations and analyzed with the NICA-EPN model for metal binding to obtain intrinsic binding parameters; also, fluorometric titrations are performed to compare the binding affinities. EEM measurements[17] with PARAFAC analysis[13,18] are conducted to study the behavior of the different fluorophores with Pb(II) additions. Finally, IR-ATR spectra are recorded to study the Pb-HA interactions.

Modeling of proton and metal binding data: the NICA-EPN model

Titration data was analyzed using the NICA isotherm for the intrinsic affinity[7] and the Elastic Polyelectrolyte Network (EPN) submodel[9] for the electrostatic contribution. In the NICA-EPN model,

the amount bound of species i per unity of mass in the presence of species j is given by

$$Q_i = g_f \sum_{k=1}^{M} \frac{n_{i,k}}{n_{1,k}} Q_{\max,k} \vartheta_{i,k}(a_1^{\text{int}},...,a_j^{\text{int}},...,a_n^{\text{int}}) + (1-g_f)\sum_{k=1}^{M} \frac{n_{i,k}}{n_{1,k}} Q_{\max,k} \vartheta_{i,k}(a_1,...,a_j,...,a_n) + Q_{i,el} \quad (1)$$

where $\vartheta_{i,k}(a_i)$ is the fraction of type k sites occupied by species i, given in the NICA isotherm by

$$\vartheta_{i,k}(a_1,...a_j,...,a_n) = \frac{\left(\bar{K}_{i,k} a_i\right)^{n_{i,k}}}{\sum_{j=1}^{n}\left(\bar{K}_{j,k} a_j\right)^{n_{j,k}}} \times \frac{\left[\sum_{j=1}^{N}\left(\bar{K}_{j,k} a_j\right)^{n_{j,k}}\right]^{p_k}}{1+\left[\sum_{j=1}^{N}\left(\bar{K}_{j,k} a_j\right)^{n_{j,k}}\right]^{p_k}} \quad (2)$$

In eqs 1 and 2, N is the number of species binding to the HA, M the number of sites, $Q_{\max}$ the total number of sites per unity of mass, $Q_{\max,k}$ the same for type k sites (assuming 1:1 binding), q_k the fraction of type k sites ($Q_{\max,k} = q_k\, Q_{\max}$), $n_{i,k}$ the nonideality parameter for species i on type k sites, ($n_{1,k}$ being for H^+), p_k is the heterogeneity parameter of type k sites and $\bar{K}_{i,k}$ is the average binding constant of species i on type k sites. Two site types are considered: low affinity (k = 1, attributed to carboxylic groups) and high affinity (k = 2, usually attributed to phenolic groups),[7,19] so M = 2, and for binding of a metal cation in the presence of protons N = 2.

As it is widely accepted, HS are actually composed of relatively small molecules and molecular fragments (as opposed to a macromolecular/polymeric view) which are entangled and/or bound by diverse forces, like hydrogen bonding, metal ion bridging, van der Waals interactions, etc. forming particles of supramolecular nature which can shrink and swell.[20,21] In the EPN model,[9] these HS particles are treated, from a purely mechano-statistical point of view, as an elastic network which can exchange ions and solvent with the surrounding solution; further, the particles are considered as divided in two fractions: an inner fraction g_f, which behaves as a gel in Donnan equilibrium with the bulk solution, and an external fraction 1 - g_f. The humic binding sites outside the gel are in equilibrium with the bulk solution, whereas those inside the gel are in equilibrium at the internal ionic activity, a_j^{int}, which is given by

$$a_j^{\text{int}} = a_j \exp\left(-F\psi_D / RT\right) \quad (3)$$

where ψ_D is the Donnan potential, a_j is the activity in the bulk and F, R and T have their usual meaning. For a 1:1 electrolyte, ψ_D results to be, from the electroneutrality condition,[9]

$$\psi_D = \frac{RT}{F}\operatorname{arcsinh}\left(\frac{g_f Q\delta\varphi_2}{2I(1-\varphi_2)}\right) \tag{4}$$

where Q is the net charge of the humic particle, δ the density of the dry humic substance (following Dinar [22] $\delta = 1.5$ g cm^{-3}), I the ionic strength, and φ_2 is the volume fraction of the HS in the gel, obtained from the swelling equilibrium condition:[9]

$$\frac{1}{v_1}\left[\chi\varphi_2^2 + \varphi_2 + \ln\left(1-\varphi_2\right)\right] + \frac{1}{v_2}\left(\varphi_2^{1/3} - \frac{2\varphi_2}{f_P}\right) + 2I\left[1-\sqrt{1+\left(\frac{g_f Q\delta\varphi_2}{2I(1-\varphi_2)}\right)^2}\right] = 0 \tag{5}$$

where v_1 is the water molar volume, v_2 is the average molar volume of a humic equivalent chain, χ is a Van Laar heat of mixing parameter and f_P is the Flory functionality,[23] which was set equal to 3. $Q_{i,el}$ is the excess amount of species i electrostatically bound in the gel phase:

$$Q_{i,el} = \left(c_i^{\text{int}} - c_i\right)\frac{g_f}{\delta\varphi_2} \tag{6}$$

where c_i^{int} and c_i are the concentrations of species i in the gel and the bulk solution, respectively. The Davies equation was employed to calculate activity coefficients throughout; it was verified that the ionic strength inside the gel was always within its validity limit ($I < 0.3$ M).

As it is well known,[7] eq 2 reduces to a Langmuir-Freundlich isotherm for non competitive (H^+) binding:

$$\vartheta_{\text{H},k}\left(a_{\text{H}}\right) = \frac{\left(\bar{K}_{\text{H},k}a_{\text{H}}\right)^{m_{\text{H},k}}}{1+\left(\bar{K}_{\text{H},k}a_{\text{H}}\right)^{m_{\text{H},k}}} \tag{7}$$

where $m_{\text{H},k} = n_{\text{H},k}\, p_k$.

Also, conditional affinity distributions can be obtained using constrained regularization methods.[24] If the proton affinity spectrum $g(\log K_H)$ is known, a conditional metal affinity distribution $f(\log K_M)$ can be estimated solving numerically the equation (assuming uncorrelated proton and metal affinity spectra):[24]

$$Q_M = Q_{\max} \int_{-\infty}^{\infty} \left[\int_{-\infty}^{\infty} \frac{K_M a_M}{1 + K_H a_H + K_M a_M} g(\log K_H) \mathrm{d} \log K_H \right] f(\log K_M) \mathrm{d} \log K_M \quad (8)$$

where Q_M is the amount of metal bound.

Materials and methods

The HAs employed were a purified Fluka humic acid (FHA) and IHSS standard Elliot soil humic acid (EHA); these HS have been characterized in the literature, as presented in Table S1, Supporting Information. Acid-base potentiometric titrations were performed following usual procedures[25] at 1 g L^{-1} HA concentration and different ionic strengths in $NaClO_4$. Pb(II)-humic potentiometric titrations also followed known procedures[10] at pHs of 4.0 and 5.5, and ionic strengths ($NaClO_4$) of 0.1 M and 0.02 M. Fluorometric titrations were performed, at a HA concentration of 20 mg L^{-1}. In order to enable comparisons, binding curves for this concentration were calculated using the fitted model parameters; some potentiometric measurements were also done, but no processed due to the low reliability of ISE measurements at low HA concentrations;[26] however, they reflected the same general tendency. Fluorescence EEMs of 20 mg L^{-1} solutions of HA alone and with increasing amounts of Pb(II) were recorded. UV-Vis spectra were also recorded to check the onset of humic flocculation. IR-ATR spectroscopy measurements of HA-Pb complexes were performed following usual techniques,[27,28] using the electrolyte spectrum as reference to obtain the difference spectra. Experimental details are given in Appendix A, Supporting Information.

The data treatment was, briefly, as follows. First from acid-base titration data the humic charge as a function of pH was computed and fitted to the NICA-EPN model, using a constrained Levenberg-Marquardt algorithm,[29] obtaining the corresponding NICA parameters as well as the EPN ones, namely χ, g_f and v_2. Then, curves of Pb(II) binding as a function of Pb(II) activity were obtained from titration data, and also fitted to the NICA-EPN model, taking the proton binding and EPN parameters from the proton experiments.

Fluorometric titration data was converted to relative fluorescence quenching, θ_F, defined as:

$$\theta_F = \frac{I_F^0 - I_F}{I_F^0 - I_F^\infty} \quad (9)$$

Here, I_F^0 is the fluorescence emission intensity in the absence of Pb(II), I_F^∞ is the intensity observed at maximum quenching and I_F is the intensity at each point. This intensity values can be taken as the intensity at the wavelength of maximum emission or as the integrated emission spectra. Both ways led to the same results. Fluorescence EEMs were converted to Raman units following Stedmon et al.,[18] processed with PARAFAC,[12,13] yielding the number of independent fluorescent phenomena, their absorption and emission spectra, and their relative concentrations (scores) in each sample. The data treatment procedures are detailed in Appendix B, Supporting information.

Results and discussion

Potentiometric titrations. Acid-base titration curve fitting to the NICA-EPN model shows very good agreement (Figure S1, Supporting Information). The intrinsic NICA parameters for proton binding are collected in Table 1, falling in the ranges reported in the literature;[19,30] also included are the total sites ($Q_{\max}$) and the electrostatic parameters g_f, χ and v_2. The proton binding constants found for low affinity sites are close to typical values for isolated carboxylic groups. For the high affinity type sites our results are close to the pK_a for phenol (9.8); it has been reported that in HS most phenolic OH groups are isolated[31,32] which is consistent with these results.

The electrostatic parameters g_f and χ are similar to those reported previously;[9] the first one represents the part of the humic particle where the electrostatic potential is on average equal to ψ_D, being about half of the binding sites, whereas a positive value for χ corresponds to a repulsive heat of mixing humic-water, which is expected because HS have a significant fraction of non polar groups. There are significant differences in v_2, quite low for EHA and high for FHA; this parameter is the molar volume of the equivalent chain segments in a network representing the humic particle, thus the results found would indicate that FHA is relatively less entangled whereas EHA would be highly entangled.

Table 1. NICA-EPN model fitting parameters

Proton binding	log $\bar{K}_{H,1}$	log $\bar{K}_{H,2}$	Q_{max}/ mol kg^{-1}	q_1	q_2	$m_{H,1}$	$m_{H,2}$	g_f	χ	v_2/ L mol^{-1}
Elliot HA	4.42	9.43	5.0	0.52	0.48	0.51	0.20	0.48	0.47	1.7
Fluka HA	4.44	9.91	5.2	0.56	0.44	0.39	0.23	0.47	0.51	10.2
Pb(II) binding	log $\bar{K}_{Pb,1}$	log $\bar{K}_{Pb,2}$	$n_{Pb,1}$	$n_{Pb,2}$	p_1	p_2		N_d[a]	R^2[b]	RMSE[c]
Elliot HA	0.55	9.8	0.80	0.49	0.70	0.40		228	0.9990	0.058
Fluka HA	0.50	5.8	0.90	0.52	0.49	0.89		209	0.9993	0.039

[a] Total data points. [b] $R^2 = 1 - \sum\left(Q_i - Q_{i,\,calc}\right)^2 \Big/ \left[\sum Q_i^2 - \left(\sum Q_i\right)^2 / N_d\right]$. [c] $\mathrm{RMSE} = \sqrt{\sum\left(Q_i - Q_{i,\,calc}\right)^2 / N_d}$.

Figure 1 shows the results for the HA-Pb titrations with good agreement; the generic NICA-Donnan (ND)[19] predicted curves being also shown for comparison. The pH dependence is similar to that reported by Milne et al.[3] and references therein. The influence of *I* has been much less studied; here it is observed that the curves at different ionic strengths merge as Pb(II) activity increases; some literature studies show similar behavior: Cu binding to Suwannee River fulvic acid,[33] Am complexation with Gohy-573 humic acid,[34] and Cu complexation with Sable silt loam HA[35]. The NICA-EPN model predicts well this dependence, whereas the generic ND curves are nearly parallel. Table 1 collects the Pb intrinsic binding parameters and the fitting quality results for the full data set fitting (proton and metal curves.

Figure 2 shows the speciation of bound Pb(II) at pH = 5.5 and *I* = 0.1 M (other cases are similar), writing eq 1 in the form:

$$Q_{Pb} = Q_{Pb,1}^{int}\left(a_H^{int}, a_{Pb}^{int}\right) + Q_{Pb,2}^{int}\left(a_H^{int}, a_{Pb}^{int}\right) + Q_{Pb,1}^{ext}\left(a_H, a_{Pb}\right) + Q_{Pb,2}^{ext}\left(a_H, a_{Pb}\right) + Q_{Pb,el} \quad (10)$$

where $Q_{\mathrm{Pb},k}^{\mathrm{int}} = g_f\left(n_{\mathrm{Pb},k} / n_{\mathrm{H},k}\right) Q_{\max,k} \vartheta_{\mathrm{Pb},k}(a_{\mathrm{Pb}}^{\mathrm{int}}, a_{\mathrm{H}}^{\mathrm{int}})$ and so on. As it is observed, most Pb is bound to high affinity sites in the activity range studied, specially for EHA. From $a_{\mathrm{Pb}} \approx 10^{-4}$ up the binding to low affinity sites shows an increase. The electrostatic binding in the gel fraction (eq 6) is negligible in all cases; note also that for FHA this contribution changes sign; this is due to inversion of the gel fraction charge caused by the Pb loading.

There are several published studies of Pb binding to HS;[3,36–42] however, direct comparisons are difficult because the different HS and conditions employed. The values of $\bar{K}_{\mathrm{Pb},k}$ found here (with the exception of high affinity sites for EHA) are within the ranges reported by Milne et al.,[3] Gustafsson,[8,40] and Tipping.[6] Puy et al.[37] reported somewhat higher values of $\log \bar{K}_{\mathrm{Pb},1}$ (4.37) and $\log \bar{K}_{\mathrm{Pb},2}$ (7.57). The high affinity constant for EHA found here is higher than the values reported by all these authors; in some studies, Pb(II) binding to soil organic matter was found to be considerably higher than predicted by current models, free Pb being about one order of magnitude lower than predicted (see Gustafsson et al.[40] and references therein). Thus, being EHA a soil HA, whereas FHA is originated from coal, the difference in their $\bar{K}_{\mathrm{Pb},2}$ values is consistent with the findings reported by Gustafsson et al.[40]

Fluorometric titrations. During titration of HA with Pb(II), fluorescent emission is quenched as Pb(II) concentration increases, until a limiting emission is reached, which does not change as Pb(II) concentration is further increased (Figure S2, Supporting Information). In all cases, the lowest emission intensity observed was taken as I_F^{∞} in eq 9 to compute θ_F. This quenching has been observed by a number of researchers and for several cations.[11,43] Along the titrations, the absorbance spectra of the HA-Pb solutions were checked. It was found to remain unchanged until the appearance of flocculation and/or precipitation, were the absorbance started to decrease (Figure S3, Supporting Information); only fluorescence measurements before this point were considered in the analysis, thus in all the results presented here the UV spectra remained constant. Figure 3 compares the results for fluorometric titrations with Pb binding curves calculated with the NICA-EPN model for EHA and FHA. The general

features are coincident with previous studies.[3,44,45] It is observed that the results are qualitatively similar but not quantitatively coincident, showing the fluorometric response a tendency to saturation at pPb ~5, which is not observed for the potentiometric curves. This behavior was also observed in preliminary experiments conducted with other cations such as Cu(II) and Mn(II) (not shown). Similar comparisons were done previously by Saar and Weber[43] who measured binding of several cations to fulvic acids, finding good correlation for Cu(II) but only poor agreement for Pb(II), and even poorer for Co(II) and Ni(II). Other studies[11,46] were instead focused on obtaining binding equilibrium constants directly from quenching data.

Excitation-Emission matrices. The EEM plots for Pb(II) binding to HA show typical shapes observed for HS[14,16,47] (Figure S4, Supporting Information). The shape changes as Pb(II) concentration increases; the emission and excitation maxima shift towards lower wavelengths in both cases, but its intensity always decreases with increasing metal concentration. The changes in shape indicate that the EEMs are linearly independent, and consequently are analyzable using PARAFAC.

After PARAFAC processing changing the number of fluorophores, N_f, between 1 and 5 it was found, in all cases, that $N_f = 3$ gave an optimal fit of the model, revealed by a low value for residual standard deviation, σ_R, and a high value for core consistency, CC, for that number (Figure S5, Supporting Information). This result is consistent with that reported in literature for IHSS reference humic substances[48] and is also consistent with measurements of fluorescence lifetime of HS, showing three distinct values.[49] Figure 4 shows contour maps of the different fluorophores for EHA and FHA, which are similar to others HA.[13,48,50] The components have been named starting from the emission maximum with the higher wavelength, the spectra showing only a small dependence with pH and ionic strength; Table S2 (Supporting Information) collects the average peak emission and excitation wavelengths for FHA and EHA. The maxima location is related to the fluorophore structure:[18,51] the higher the degree of conjugation, the higher the excitation wavelength; this suggests that the A component is the more

aromatic, with aromaticity decreasing in the B and C components. The component C is also observed in fulvic acids.[52] The three have spectral characteristics consistent with the operationally defined humic acids by Chen et al.[53] based on pyrolysis results.[54] The quenching efficiency for these components lies in the same order: the more aromatic is more efficiently quenched. In similar studies with dissolved organic matter and aquatic HS, 13 fluorophores were reported,[55] including aminoacid-like components with emission $\lambda_{em,max} \leq 350$ nm; one of such fluorophores (tyrosine-like) was found[56] to give high deviation from linearity in inner filter effects for A_{254} (the absorbance at 254 nm) > 0.3, all the rest showed low deviations up to $A_{254} \cong 1.0$. In this study, no such fluorophore is found; moreover, the fluorescence titrations are treated as relative values (eq 9) and the HA concentration and the full absorbance spectra are constant in the measurements, thus the correction should be the same for all data, even being nonlinear. Consequently, the PARAFAC resulting spectra were corrected for inner filter effects. In view of the above considerations, the results shown in Figure 5 should be considered as semiquantitative.

Figure 5 present typical results for the scores (concentrations) of each fluorophore as a function of total Pb(II) concentration, c^0_{Pb}. Other results are presented in Figures S6 and S7 (Supporting Information). It is seen that component A has the higher scores and shows greater quenching, followed in both aspects by B and then C. Usually, the behavior is similar for all three components; in some cases, the component C shows no observable quenching. No essential differences are found between components; similar results were found by Yamashita and Jaffé.[47]

IR-ATR spectra. In Figure 6 the spectra of EHA in the absence and presence of Pb(II) are shown; as detailed in Appendix B (Supporting Information) the 4000-3000 cm^{-1} was recorded with lower sensitivity due to water band saturation, thus presenting higher noise. The bare EHA spectrum is typical of HS,[2] having relatively broad bands resulting from the multiple chemical environments of the absorbing groups. Here, we will discuss mainly the carboxylic C=O stretching at 1720 cm^{-1} and the carboxylate bands at 1585 (ν_a, asymmetric stretching) and 1380 cm^{-1} (ν_s, symmetric);[57,58] these bands

are marked in the figure. Also, a sharp band is observed at *ca*. 1105 cm^{-1}, attributed to C-O stretching of polysaccharide-like substances[59] and a weak band at *ca*. 1260 cm^{-1} attributable to phenol groups.[60] Finally, the OH stretching region shows a negative band due to differences in OH absorption between the HA solution and the electrolyte reference.

Two spectra with Pb in different concentrations are shown; using NICA-EPN parameters, the metal loadings are estimated as 0.36 and 2.4 mol kg^{-1}, thus these can be considered as representative of low and high loadings, respectively. In the low loading case, the carboxylic band decreases, whereas the carboxylate bands increase and shift to 1564 and 1386 cm^{-1}, respectively, indicating that carboxylate groups are involved in binding; the other bands mentioned do not change, indicating that OH groups are not involved. Under high loading, those changes appear enhanced, except for ν_s, where a sharp increase is found and new band arises at 1350 cm^{-1}; the sharp increase has been observed in other cases,[28,59] whereas the new band indicates a different carboxylate binding mode. According to Nakamoto,[58] the difference $\Delta=\nu_a-\nu_s$ is indicative of the binding mode, a decrease being attributable to a chelate (metal bound to both O atoms) or a bridging complex (one metal bound to each O atom); here Δ decreases from 205 to 178 cm^{-1} at low loading, which is likely due to chelate formation, whereas the new band at high loading shows Δ=208 cm^{-1}, a small increase which could be indicative of monodentate binding. The C-O bands again do not show changes, whereas in the OH region a small increase is observed, which could be attributable to OH^- ions coordinating the Pb ions; involvement of HA OH groups in binding would result in a decrease due to deprotonation. Thus, we conclude that Pb binding to the HA proceeds via the carboxylate groups in different modes depending on metal loading, without appreciable involvement of OH groups.

Affinity spectra. Figure 7 shows the affinity spectrum for Pb(II) binding to EHA corresponding to the NICA fitting results shown in Table 1, compared with the conditional spectra for fluorometric measurements obtained solving numerically eq 8; similar results are obtained for FHA (Figure S8, Supporting Information); Figure S9 (Supporting Information) shows the NICA affinity distributions for

protons. These are bimodal distributions with peaks at log K_{Pb} values ~0.5 for the low affinity sites, being for high affinity 5.8 for FHA and 9.8 for EHA. On the other hand, fluorometric results show monomodal distributions peaking at ~5 for FHA and ~6-7 for EHA, roughly coincident with the higher affinity peak from the potentiometric experiments. This suggests (considering also IR results) that fluorescent quenching is sensing only high affinity sites for Pb(II), whereas potentiometric analysis finds two types. Comparison of potentiometric and fluorometric measurements has been conducted by several researchers,[4,43,61,62] usually finding that metal binding quenches the HS fluorescence; however, it was noted that both techniques do not sense the same complexation phenomena:[4] for Cu binding to fulvic acid, it was observed that the two measurements agreed only at low levels of copper loading,[61] which is consistent with our findings. Also, Saar and Weber found poor agreement between potentiometric and fluorometric measurements for Pb.[43] These binding sites are expected to be, given the IR results, carboxylates; this is also consistent with the fact that carboxylate groups are known to form stable complexes with Pb(II)[63] whereas phenol groups are not expected to bind Pb(II) at the present pH values.[64] There are a number of studies which seek to obtain binding constants between metal cations and humic substances from fluorescence measurements, based on the assumptions of 1:1 binding and that fluorescence was detecting all types of binding sites.[46] However, as already observed by Senesi,[4] the two techniques are not equivalent and, as found here, fluorometry senses only the strongly binding sites. Therefore, the binding constants obtained exclusively through fluorometry should be considered valid only in the context of this technique.

Fluorescence quenching. Quenching of fluorescence can be caused by several mechanisms, mainly dynamic (collisional) and static (complex formation).[51] For single fluorophores, the Stern-Volmer plot, a graphic of I_F^0/I_F as a function of the total quencher concentration, is useful to reveal the type of quenching taking place.[51] For HS, their complex nature introduces difficulties because the observed emission is the result of the combination of several fluorescence phenomena. Here, we treat the PARAFAC components as independent fluorophores to analyze the quenching behavior. In most cases,

the Stern-Volmer plots show an upward curvature (Figure S10, Supporting Information); for simple cases, this is indicative of mixed static-dynamic quenching;[51] however dynamic (collisional) quenching is usually important at concentrations several orders of magnitude higher.[65] Furthermore, attempts to deduce quenching parameters by usual methods[51] from these plots lead to unreasonably high values for the dynamic quenching constant. Thus we conclude that static quenching is present in this case, as found before for other metal-HS systems.[4] The effect could be due to different causes;[51] for HS it has been attributed to intersystem crossing;[4] that is, enhanced transference from the singlet excited state to the triplet ground state. Aromatic carboxylic acids show usually this type of quenching.[4,46,61,66] However, in the case of HS this is not necessarily true: some studies[66] show that complexes of model compounds with heavy metal ions (such as Tb(III)) show quenching whereas binding of the same cation to HS does not. Furthermore, a molecular quenching mechanism such as intersystem crossing would require the carboxylic groups to be directly bound to the fluorescent aromatic groups, but this is not necessarily the case: on one hand not all the fluorescent aromatic groups would have a carboxylic substituent, and on the other not every carboxylate would be attached to a fluorophore group.[1,2,4] Thus, we propose as an alternative quenching mechanism the aggregation of humic molecules induced by Pb(II) binding. Quenching by dimerization of aromatic and highly conjugated substances is well known[67,68] and shows increasing efficiency at higher wavelengths, as it is observed here; on the other hand, aggregation of HS by cation binding is well known.[69] Starting from this assumption, the quenching can be rationalized in the following way, considering the process schematically depicted in Figure 8. When Pb(II) is added, it first binds in bidentate form promoting aggregation by bridging two humic molecules; one or several metal ions are expected to participate in the bridging. This process corresponds to the high affinity part of the spectrum, which is thus assumed to correspond to bidentate complexation, but not necessarily all Pb(II) bound in this way participate in bridging. Further increase in Pb(II) concentration results in singly coordinated binding to carboxylate groups, corresponding to the low affinity part.

The process for the high affinity sites, which causes quenching, can be written as

$$2\mathrm{HA} + n\mathrm{Pb}^{2+} \rightleftharpoons (\mathrm{HA})_2\mathrm{Pb}_n \tag{11}$$

where n is the average number of Pb^{2+} ions bridging humic molecules, considering the HA heterogeneity. The reaction will have a conditional equilibrium constant given by

$$K = \frac{[(\mathrm{HA})_2\mathrm{Pb}_n]}{[\mathrm{HA}]^2 c_{\mathrm{Pb}}^n} \tag{12}$$

where c_{Pb} is the free Pb(II) concentration. Now, if it is assumed that free HA molecules show emission whereas those bound do not, it can be written for the total fluorophore concentration F_0:[51]

$$F_0 = F + 2C \tag{13}$$

where F is the concentration of free fluorophores and C is the complexed fluorophores (not emitting) concentration. Identifying F with [HA] and C with $[HA_2Pb_n]$, it can be found from eqs 12 and 13, and taking into account that fluorescent intensity is proportional to fluorophore concentration, that

$$\frac{I_F^0}{I_F} = \frac{F_0}{F} = \frac{1 + \sqrt{1 + 8KF_0 c_{\mathrm{Pb}}^n}}{2} \tag{14}$$

Figure 9 shows the fit of FHA fluorophore scores (in Stern-Volmer form) to eq 14 using a common n value for all curves, and different values for the product KF_0. The free Pb(II) concentration are obtained from the potentiometric results with the Davies equation for activity coefficients. A good fitting is found in general, the C component in some cases show a less satisfactory fitting, but it can be due to its lower intensity, resulting in higher errors. EHA data shows similar fitting (Figure S11, Supporting Information). All FHA curves are fit with n = 1.6, whereas EHA fits with n = 1.3. Unfortunately, K and F_0 cannot be separated, because the many unknown factors; the resulting values for their product are presented in Table S3, Supporting Information.

Thus, we conclude that fluorescence quenching is consistent with metal-induced aggregation of HS; this aggregation proceeds at a molecular scale, to be distinguished of precipitation, however, more experimental information is needed to confirm this mechanism. Other spectroscopic studies are consistent with the present findings. Xia et al.[70] studied by X-ray absorption the interaction of Pb(II) with a humic extract from a silt loam soil suggesting the presence of two C atoms in the second

coordination shell, which would indicate bidentate binding. A study by EPR measurements combined with DFT analysis is consistent with a structure of Pb (II) bound to two carboxylates.[71]

Concluding, the NICA-EPN model here introduced describes adequately the binding of proton and Pb(II) to humic acids; fluorescence quenching has a different dependence with Pb concentration compared with potentiometric titrations: it is proposed that the addition of Pb(II) causes dimerization (or aggregation) of humic molecules. Thus, fluorescent quenching senses multiligand Pb(II) binding (which, from IR results, should be a chelate type complex), and the second site type (with lower affinity) observed in potentiometric measurements is proposed be due to 1:1 binding.

Acknowledgments. The authors wish to thank Dr. A. Olivieri for his assistance with PARAFAC processing. The authors gratefully acknowledge financial support from the Universidad de Buenos Aires (UBACYT 2008-2010 X148), the Consejo Nacional de Investigaciones Científicas y Técnicas and the Agencia Nacional de Promoción Científica y Tecnológica (grant Nº 06-12467). F. V. M. is a member of the Carrera del Investigador Científico of CONICET.

Supporting Information Available. Additional figures and tables. Appendix A details the experimental procedures, and Appendix B does the same for data analysis. This material is available free of charge via the Internet at http://pubs.acs.org.

FIGURE CAPTIONS

Figure 1. Pb(II) binding curves at different pH and ionic strengths for Elliot soil humic acid (a) and purified Fluka humic acid (b). The dotted lines are the NICA-Donnan predicted curves with the generic recommended parameters of Milne et al.[3] 1 g L^{-1} HA in $NaClO_4$ at the ionic strengths shown.

Figure 2. Speciation of Pb(II) binding at pH = 5.5 and I = 0.1 M in $NaClO_4$ (1 g L^{-1} HA) for Elliot soil humic acid (a) and purified Fluka humic acid (b). The closed symbols (total and high affinity binding) correspond to the left side scale, and open symbols (low affinity and electrostatic binding) to the right side scale.

Figure 3. Amount of metal bound (closed symbols) and relative fluorescence quenching (open symbols) for simultaneous potentiometric and fluorescence titration of EHA (a) and FHA (b) with Pb(II). 20 mg L^{-1} HA in $NaClO_4$ at the ionic strengths shown.

Figure 4. Fluorescence components as obtained from PARAFAC. (Top) Elliot soil humic acid, pH = 4.0; I = 0.02 M; (bottom) Purified Fluka humic acid, pH = 5.5, I = 0.1 M. Blue is zero intensity, red is maximum (arbitrary scale). 20 mg L^{-1} HA in $NaClO_4$.

Figure 5. Scores of the fluorescence components (shown in Figure 3) deduced form PARAFAC as a function of total Pb(II) concentration, for 20 mg L^{-1} FHA at pH = 5.5, I = 0.02 M ($NaClO_4$).

Figure 6. ATR-IR spectra of Elliot soil HA (0.28 g L^{-1}) in the absence and in the presence of Pb(II) at different concentrations. pH = 5.5, I = 0.1 M ($NaClO_4$). See text for details.

Figure 7. Affinity spectrum found for EHA by NICA fitting (solid lines) and conditional spectra found from analysis based on eq 8 of fluorometric quenching experiments (dashed lines).

Figure 8. Simplified scheme of the humic-Pb(II) interaction. In the first stage (high affinity sites) the Pb^{2+} ions promote aggregation of humic molecules through bridging; the Pb ions bind to carboxylate groups in chelate form as indicated by IR results. In the second stage, 1:1 binding takes place yielding the low affinity sites; mainly single bond Pb binding is assumed, as suggested by IR results.

Figure 9. Stern-Volmer plots as a function of free Pb(II) concentrations for FHA fluorophores (symbols). Lines show the fitting to eq 14.

REFERENCES

(1) Senesi, N.; Loffredo, E. The Chemistry of Soil Organic Matter. In *Soil Physical Chemistry*; Sparks, D. L., Ed.; CRC Press: Boca Raton, Fl, 1998; pp. 239–370.

(2) Baldock, J. A.; Nelson, P. N. Soil Organic Matter. In *Handbook of Soil Science*; M. L. Sumner, ed.; CRC: Boca Raton, Fl, 1999; pp. B75–B84.

(3) Milne, C. J.; Kinniburgh, D. G.; van Riemsdijk, W. H.; Tipping, E. Generic NICA−Donnan Model Parameters for Metal-Ion Binding by Humic Substances. *Environ. Sci. Technol.* **2003**, *37*, 958–971.

(4) Senesi, N. Molecular and quantitative aspects of the chemistry of fulvic acid and its interactions with metal ions and organic chemicals: Part II. The fluorescence spectroscopy approach. *Anal. Chim. Acta* **1990**, *232*, 77–106.

(5) Cabaniss, S. E. Forward Modeling of Metal Complexation by NOM: I. A priori Prediction of Conditional Constants and Speciation. *Environ. Sci. Technol.* **2009**, *43*, 2838–2844.

(6) Tipping, E. Humic ion-binding model VI: An improved description of the interactions of protons and metal ions with humic substances. *Aquat. Geochem.* **1998**, *4*, 3–48.

(7) Kinniburgh, D. G.; Van Riemsdijk, W. H.; Koopal, L. K.; Borkovec, M.; Benedetti, M. F.; Avena, M. J. Ion binding to natural organic matter: Competition, heterogeneity, stoichiometry and thermodynamic consistency. *Colloid Surface A* **1999**, *151*, 147–166.

(8) Gustafsson, J. P. Modeling the acid-base properties and metal complexation of humic substances with the Stockholm Humic Model. *J. Colloid Interf. Sci.* **2001**, *244*, 102–112.

(9) Orsetti, S.; Andrade, E. M.; Molina, F. V. Modeling ion binding to humic substances: Elastic polyelectrolyte network model. *Langmuir* **2010**, *26*, 3134–3144.

(10) Benedetti, M. F.; Milne, C. J.; Kinniburgh, D. G.; Van Riemsdijk, W. H.; Koopal, L. K. Metal Ion Binding to Humic Substances: Application of the Non-Ideal Competitive Adsorption Model. *Environ. Sci. Technol.* **1995**, *29*, 446–457.

(11) Smith, D. S.; Kramer, J. R. Multisite metal binding to fulvic acid determined using multiresponse fluorescence. *Anal. Chim. Acta* **2000**, *416*, 211–220.

(12) Bro, R. Exploratory study of sugar production using fluorescence spectroscopy and multi-way analysis. *Chemom. Intell. Lab. Syst.* **1999**, *46*, 133–147.

(13) Stedmon, C. A.; Bro, R. Characterizing dissolved organic matter fluorescence with parallel factor analysis: A tutorial. *Limnol. Oceanogr.: Methods* **2008**, *6*, 572–579.

(14) Ohno, T.; Amirbahman, A.; Bro, R. Parallel Factor Analysis of Excitation–Emission Matrix Fluorescence Spectra of Water Soluble Soil Organic Matter as Basis for the Determination of Conditional Metal Binding Parameters. *Environ. Sci. Technol.* **2008**, *42*, 186–192.

(15) Santín, C.; Yamashita, Y.; Otero, X.; Álvarez, M.; Jaffé, R. Characterizing humic substances from estuarine soils and sediments by excitation-emission matrix spectroscopy and parallel factor analysis. *Biogeochemistry* **2009**, *96*, 131–147.

(16) Ishii, S. K. L.; Boyer, T. H. Behavior of Reoccurring PARAFAC Components in Fluorescent Dissolved Organic Matter in Natural and Engineered Systems: A Critical Review. *Environ. Sci. Technol.* **2012**, *46*, 2006–2017.

(17) Patel-Sorrentino, N.; Mounier, S.; Benaim, J. Y. Excitation-emission fluorescence matrix to study pH influence on organic matter fluorescence in the Amazon basin rivers. *Water Res.* **2002**, *36*, 2571–2581.

(18) Stedmon, C. A.; Markager, S.; Bro, R. Tracing dissolved organic matter in aquatic environments using a new approach to fluorescence spectroscopy. *Mar. Chem.* **2003**, *82*, 239–254.

(19) Milne, C. J.; Kinniburgh, D. G.; Tipping, E. Generic NICA-Donnan Model Parameters for Proton Binding by Humic Substances. *Environ. Sci. Technol.* **2001**, *35*, 2049–2059.

(20) Clapp, C. E.; Hayes, M. H. B.; Simpson, A. J.; Kingery, W. L. Chemistry of soil organic matter. In *Chemical Processes in Soils*; Tabatabai, M. A.; Sparks, D. L., Eds.; Soil Science Society of America: Madison, Wisconsin, 2005; pp. 1–150.

(21) Duval, J. F. L.; Wilkinson, K. J.; Van Leeuwen, H. P.; Buffle, J. Humic Substances Are Soft and Permeable: Evidence from Their Electrophoretic Mobilities. *Environ. Sci. Technol.* **2005**, *39*, 6435–6445.

(22) Dinar, E.; Mentel, T. F.; Rudich, Y. The density of humic acids and humic like substances (HULIS) from fresh and aged wood burning and pollution aerosol particles. *Atmos. Chem. Phys.* **2006**, *6*, 5213–5224.

(23) Flory, P. J. Statistical Mechanics of Swelling of Network Structures. *J. Chem. Phys.* **1950**, *18*, 108–111.

(24) Orsetti, S.; Andrade, E. M.; Molina, F. V. Application of a constrained regularization method to extraction of affinity distributions: Proton and metal binding to humic substances. *J. Colloid Interf. Sci.* **2009**, *336*, 377–387.

(25) Milne, C. J.; Kinniburgh, D. G.; De Wit, J. C. M.; Van Riemsdijk, W. H.; Koopal, L. K. Analysis of proton binding by a peat humic acid using a simple electrostatic model. *Geochim. Cosmochim. Acta* **1995**, *59*, 1101–1112.

(26) Christl, I.; Metzger, A.; Heidmann, I.; Kretzschmar, R. Effect of Humic and Fulvic Acid Concentrations and Ionic Strength on Copper and Lead Binding. *Environ. Sci. Technol.* **2005**, *39*, 5319–5326.

(27) Tejedor-Tejedor, M. I.; Anderson, M. A. "In situ" ATR-Fourier transform infrared studies of the goethite (α-FeOOH)-aqueous solution interface. *Langmuir* **1986**, *2*, 203–210.

(28) Orsetti, S.; Quiroga, M. M.; Andrade, E. M. Binding of Pb(II) in the system humic acid/goethite at acidic pH. *Chemosphere* **2006**, *65*, 2313–2321.

(29) Lourakis, M. Levenberg-Marquardt in C/C++ http://www.ics.forth.gr/~lourakis/levmar/ (accessed Feb 24, 2013).

(30) Matynia, A.; Lenoir, T.; Causse, B.; Spadini, L.; Jacquet, T.; Manceau, A. Semi-empirical proton binding constants for natural organic matter. *Geochimica et Cosmochimica Acta* **2010**, *74*, 1836–1851.

(31) Deshmukh, A. P.; Pacheco, C.; Hay, M. B.; Myneni, S. C. B. Structural environments of carboxyl groups in natural organic molecules from terrestrial systems. Part 2: 2D NMR spectroscopy. *Geochimica et Cosmochimica Acta* **2007**, *71*, 3533–3544.

(32) Kirishima, A.; Ohnishi, T.; Sato, N.; Tochiyama, O. Determination of the phenolic-group capacities of humic substances by non-aqueous titration technique. *Talanta* **2009**, *79*, 446–453.

(33) Mcknight, D. M.; Wershaw, R. L. Complexation of Copper by Fulvic Acid from the Suwannee River- Effect of Counter-Ion Concentration. In *Humic Substances in the Suwannee River, Georgia: Interactions, Properties, and Proposed Structures*; Averett, R. C.; Leenheer, J. A.; McKnight, D. M.; Thorn, K. A., Eds.; U.S. Geological Survey, 1989; pp. 59–79.

(34) Czerwinski, K. R.; Kim, J. I.; Rhee, D. S.; Buckau, G. Complexation of trivalent actinide ions (Am3+, Cm3+) with humic acid: The effect of ionic strength. *Radiochimica Acta* **1996**, *72*, 179–187.

(35) Robertson, A. P. Ph. D. Dissertation, Stanford University, CA, 1996.

(36) Chakraborty, P.; Chakrabarti, C. L. Competition from Cu(II), Zn(II) and Cd(II) in Pb(II) binding to Suwannee River Fulvic Acid. *Water, Air, and Soil Pollution* **2008**, *195*, 63–71.

(37) Puy, J.; Galceran, J.; Huidobro, C.; Companys, E.; Samper, N.; Garcés, J. L.; Mas, F. Conditional affinity spectra of Pb2+-humic acid complexation from data obtained with AGNES. *Environmental Science and Technology* **2008**, *42*, 9289–9295.

(38) Quan, G.; Yan, J. Binding constants of lead by humic and fulvic acids studied by anodic stripping square wave voltammetry. *Russian Journal of Electrochemistry* **2010**, *46*, 90–94.

(39) David, C.; Mongin, S.; Rey-Castro, C.; Galceran, J.; Companys, E.; Garcés, J. L.; Salvador, J.; Puy, J.; Cecilia, J.; Lodeiro, P.; Mas, F. Competition effects in cation binding to humic acid: Conditional affinity spectra for fixed total metal concentration conditions. *Geochimica et Cosmochimica Acta* **2010**, *74*, 5216–5227.

(40) Gustafsson, J. P.; Tiberg, C.; Edkymish, A.; Kleja, D. B. Modelling lead(II) sorption to ferrihydrite and soil organic matter. *Environ. Chem.* **2011**, *8*, 485–492.

(41) Ahmetli, G.; Yel, E.; Deveci, H.; Bravo, Y.; Bravo, Z. Investigation of Pb(II) adsorption onto natural and synthetic polymers. *Journal of Applied Polymer Science* **2012**, *125*, 716–724.

(42) Lin, D.; Tian, X.; Li, T.; Zhang, Z.; He, X.; Xing, B. Surface-bound humic acid increased Pb2+ sorption on carbon nanotubes. *Environmental Pollution* **2012**, *167*, 138–147.

(43) Saar, R. A.; Weber, J. H. Comparison of spectrofluorometry and ion-selective electrode potentiometry for determination of complexes between fulvic acid and heavy-metal ions. *Anal. Chem.* **1980**, *52*, 2095–2100.

(44) Liu, A.; Gonzalez, R. D. Modeling adsorption of copper(II), cadmium(II) and lead(II) on purified humic acid. *Langmuir* **2000**, *16*, 3902–3909.

(45) Fasfous, I. I.; Chakrabarti, C. L.; Murimboh, J.; Yapici, T. Complexation of lead in model solutions of humic acid: Heterogeneity and effects of competition with copper, nickel, and zinc. *Environ. Chem.* **2006**, *3*, 276–285.

(46) Ryan, D. K.; Weber, J. H. Fluorescence quenching titration for determination of complexing capacities and stability constants of fulvic acid. *Anal. Chem.* **1982**, *54*, 986–990.

(47) Yamashita, Y.; Jaffé, R. Characterizing the Interactions between Trace Metals and Dissolved Organic Matter Using Excitation−Emission Matrix and Parallel Factor Analysis. *Environmental Science & Technology* **2008**, *42*, 7374–7379.

(48) He, Z.; Ohno, T.; Cade-Menun, B. J.; Erich, M. S.; Honeycutt, C. W. Spectral and Chemical Characterization of Phosphates Associated with Humic Substances. *Soil Sci. Soc. Am. J.* **2006**, *70*, 1741.

(49) Hemmingsen, S. L.; McGown, L. B. Phase-resolved fluorescence spectral and lifetime characterization of commercial humic substances. *Appl. Spectrosc.* **1997**, *51*, 921–929.

(50) Kowalczuk, P.; Cooper, W. J.; Durako, M. J.; Kahn, A. E.; Gonsior, M.; Young, H. Characterization of dissolved organic matter fluorescence in the South Atlantic Bight with use of PARAFAC model: Relationships between fluorescence and its components, absorption coefficients and organic carbon concentrations. *Mar. Chem.* **2010**, *118*, 22–36.

(51) Lakowicz, J. R. *Principles of Fluorescence Spectroscopy*; 3rd ed.; Springer: New York, 2006.

(52) Park, J.-H. Spectroscopic characterization of dissolved organic matter and its interactions with metals in surface waters using size exclusion chromatography. *Chemosphere* **2009**, *77*, 485–494.

(53) Chen, W.; Westerhoff, P.; Leenheer, J. A.; Booksh, K. Fluorescence Excitation−Emission Matrix Regional Integration to Quantify Spectra for Dissolved Organic Matter. *Environ. Sci. Technol.* **2003**, *37*, 5701–5710.

(54) Leenheer, J. A.; Croué, J.-P. Peer Reviewed: Characterizing Aquatic Dissolved Organic Matter. *Environ. Sci. Technol.* **2003**, *37*, 18A–26A.

(55) Cory, R. M.; McKnight, D. M. Fluorescence Spectroscopy Reveals Ubiquitous Presence of Oxidized and Reduced Quinones in Dissolved Organic Matter. *Environ. Sci. Technol.* **2005**, *39*, 8142–8149.

(56) Miller, M.; Simone, B.; McKnight, D.; Cory, R.; Williams, M.; Boyer, E. New light on a dark subject: comment. *Aquatic Sciences - Research Across Boundaries* **2010**, *72*, 269–275.

(57) Hay, M. B.; Myneni, S. C. B. Structural environments of carboxyl groups in natural organic molecules from terrestrial systems. Part 1: Infrared spectroscopy. *Geochim. Cosmochim. Acta* **2007**, *71*, 3518–3532.

(58) Nakamoto, K. *Infrared and Raman Spectra of Inorganic and Coordination Compounds, Applications in Coordination, Organometallic, and Bioinorganic Chemistry*; Part B.; John Wiley & Sons: Hoboken, NJ, 2009.

(59) Zhang, J.; Dai, J.; Wang, R.; Li, F.; Wang, W. Adsorption and desorption of divalent mercury (Hg2+) on humic acids and fulvic acids extracted from typical soils in China. *Colloids and Surfaces A: Physicochemical and Engineering Aspects* **2009**, *335*, 194–201.

(60) Coates, J. Interpretation of Infrared Spectra. A Practical Approach. In *Encyclopedia of Analyical Chemistry*; Meyers, R. A., Ed.; John Wiley & Sons: Chichester, UK, 2000; pp. 10815–10837.

(61) Cabaniss, S. E.; Shuman, M. S. Combined ion selective electrode and fluorescence quenching detection for copper-dissolved organic matter titrations. *Anal. Chem.* **1986**, *58*, 398–401.

(62) Marang, L.; Reiller, P. E.; Eidner, S.; Kumke, M. U.; Benedetti, M. F. Combining Spectroscopic and Potentiometric Approaches to Characterize Competitive Binding to Humic Substances. *Environmental Science & Technology* **2008**, *42*, 5094–5098.

(63) Alcock, N. W.; Tracy, V. M.; Waddington, T. C. Acetates and acetato-complexes. Part 2. Spectroscopic studies. *J. Chem. Soc., Dalton Trans.* **1976**, 2243–2246.

(64) Cabaniss, S. E. Quantitative Structure−Property Relationships for Predicting Metal Binding by Organic Ligands. *Environ. Sci. Technol.* **2008**, *42*, 5210–5216.

(65) Steiner, R. F.; Kirby, E. P. Interaction of the ground and excited states of indole derivatives with electron scavengers. *J. Phys. Chem.* **1969**, *73*, 4130–4135.

(66) Kumke, M. U.; Eidner, S. Fluorescence and Energy Transfer Processes of Humic Substances and Related Model Compounds in Terbium Complexes. In *Humic Substances: Molecular Details and Applications in Land and Water Conservation*; Ghabbour, E. A.; Davies, G., Eds.; Taylor & Francis, 2005; pp. 131–152.

(67) Lavorel, J. Influence of Concentration on the Absorption Spectrum and the Action Spectrum of Fluorescence of Dye Solutions. *J. Phys. Chem.* **1957**, *61*, 1600–1605.

(68) West, W.; Pearce, S. The Dimeric State of Cyanine Dyes. *J. Phys. Chem.* **1965**, *69*, 1894–1903.

(69) Senesi, N.; Loffredo, E. Metal Ion Complexation by Soil Humic Substances. In *Chemical Processes in Soils*; Tabatabai, M. A.; Sparks, D. L., Eds.; SSSA Book Series; Soil Science Society of America: Madison, Wisconsin, 2005; pp. 563–617.

(70) Xia, K.; Bleam, W.; Helmke, P. A. Studies of the nature of Cu2+ and Pb2+ binding sites in soil humic substances using X-ray absorption spectroscopy. *Geochim. Cosmochim. Acta* **1997**, *61*, 2211–2221.

(71) Witwicki, M.; Jerzykiewicz, M.; Jaszewski, A. R.; Jezierska, J.; Ozarowski, A. Influence of Pb(II) Ions on the EPR Properties of the Semiquinone Radicals of Humic Acids and Model Compounds: High Field EPR and Relativistic DFT Studies. *J. Phys. Chem. A* **2009**, *113*, 14115–14122.

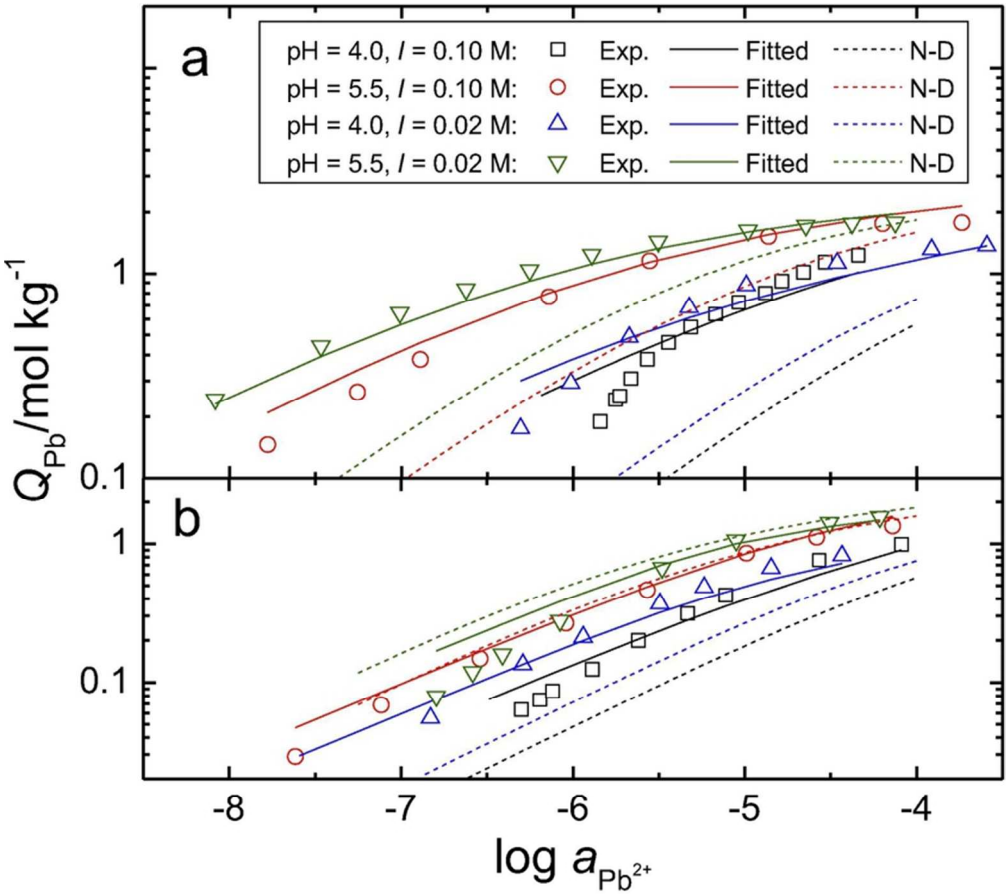

Figure 1
71x63mm (300 x 300 DPI)

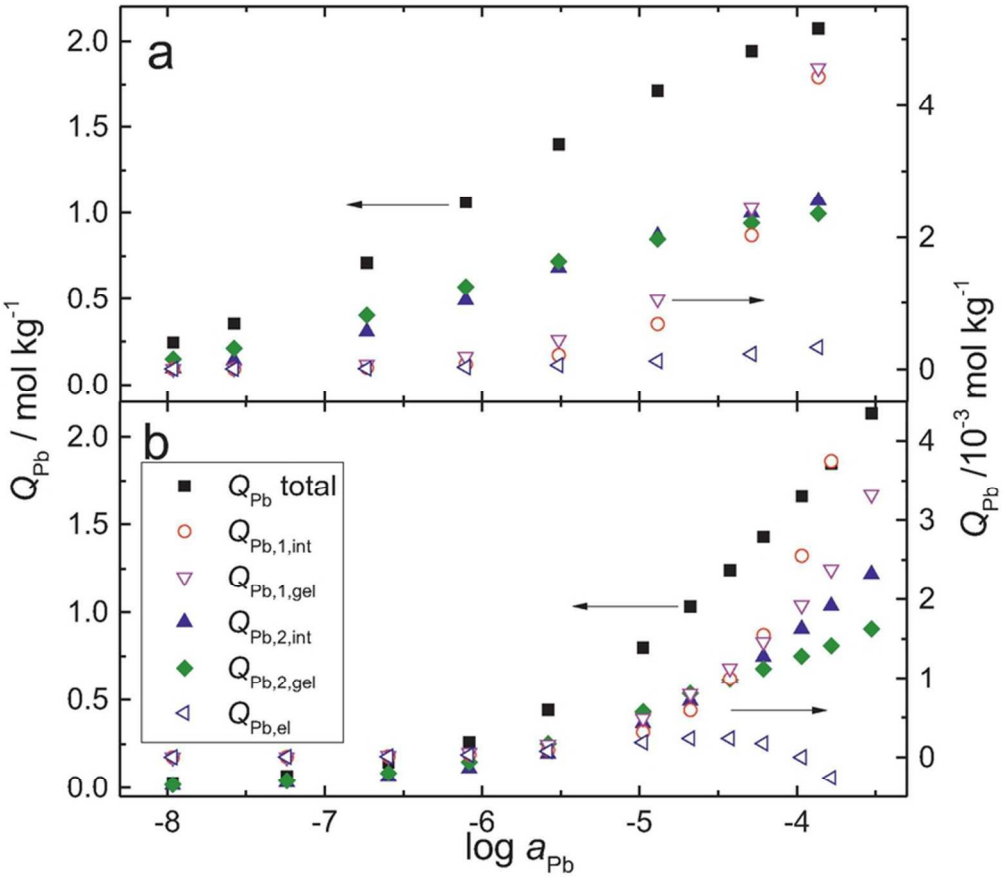

Figure 2
70x61mm (300 x 300 DPI)

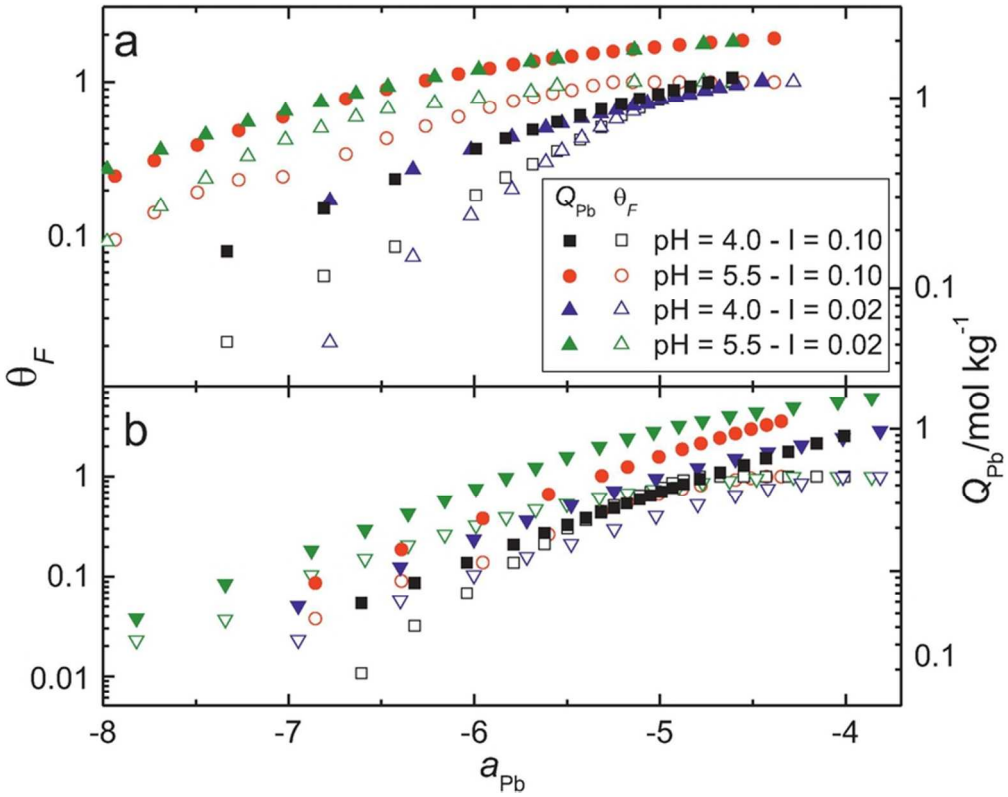

Figure 3
72x57mm (300 x 300 DPI)

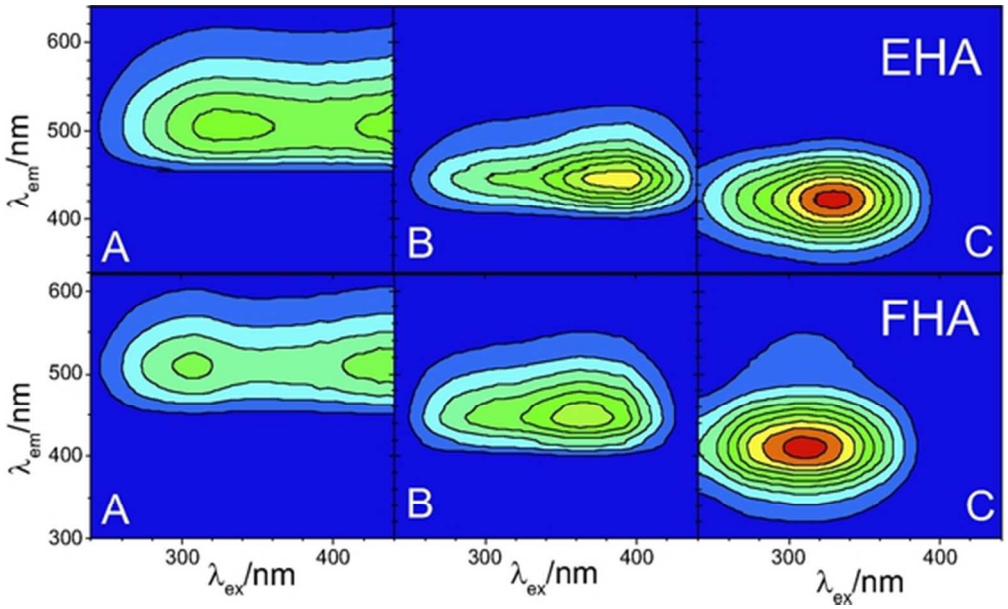

Figure 4
50x30mm (300 x 300 DPI)

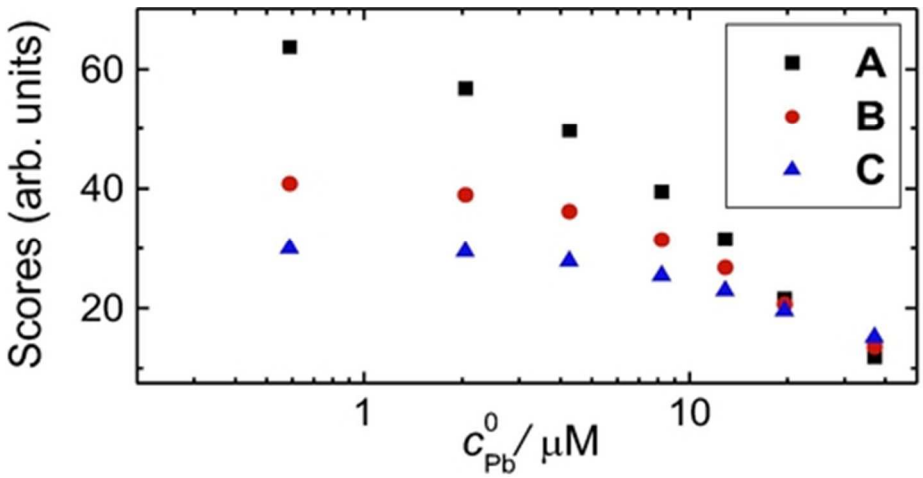

Figure 5
38x19mm (300 x 300 DPI)

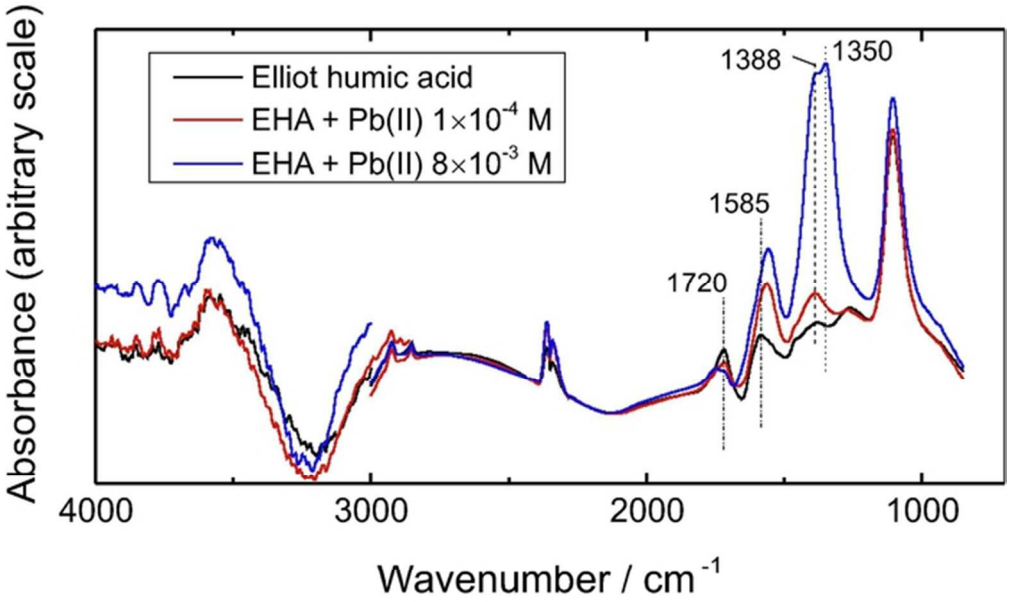

Figure 6
58x39mm (300 x 300 DPI)

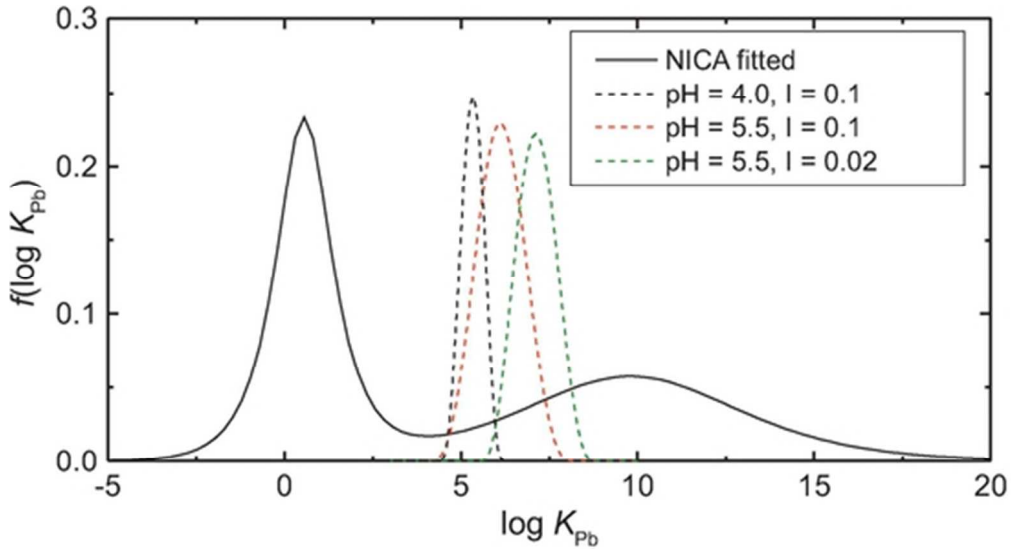

Figure 7
46x25mm (300 x 300 DPI)

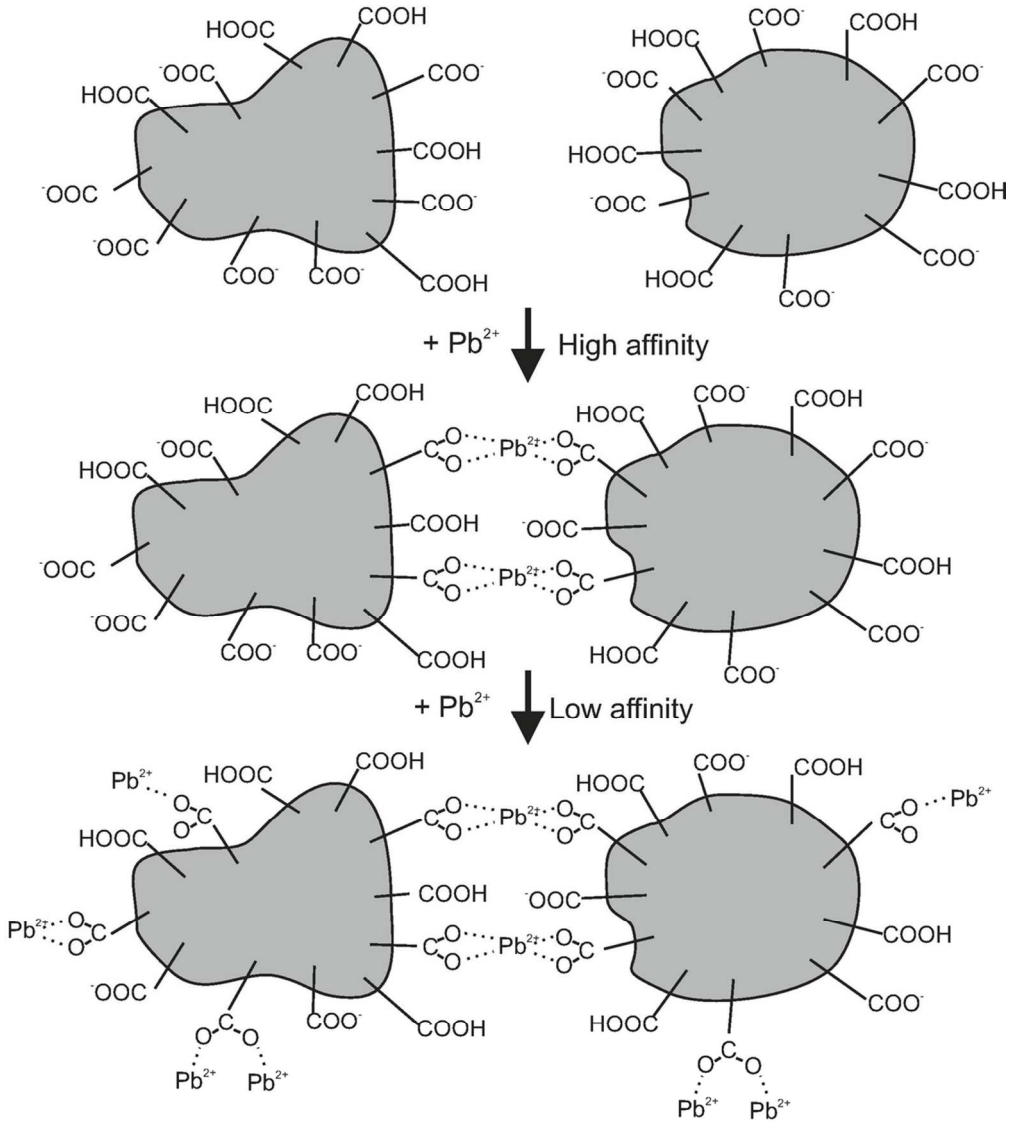

Figure 8
101x113mm (300 x 300 DPI)

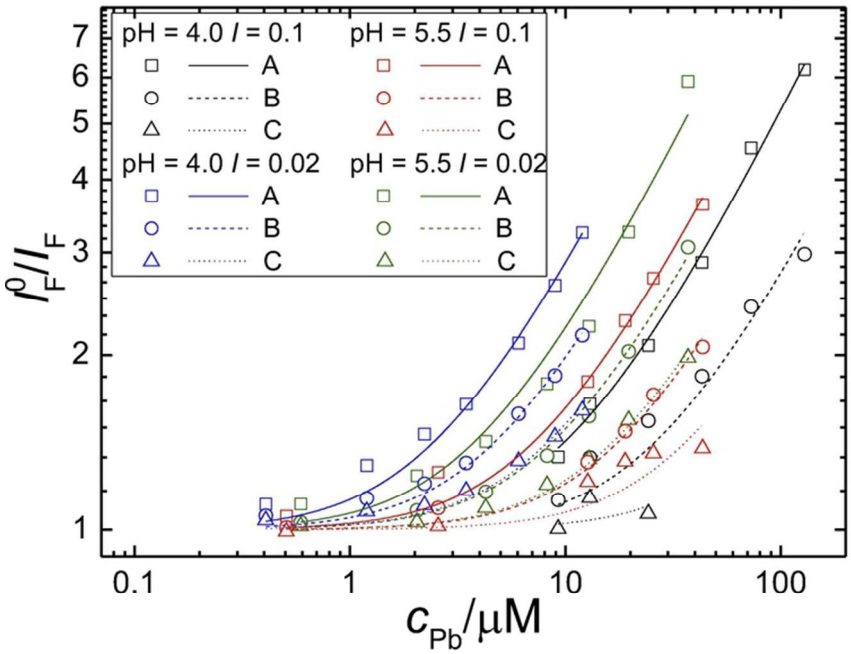

Figure 9
75x51mm (300 x 300 DPI)

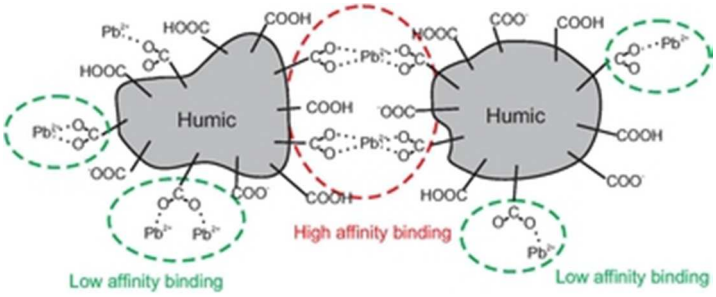

TOC Art
29x12mm (300 x 300 DPI)